T1 mapping and feature tracking imaging of left ventricular extracellular remodeling in severe aortic stenosis

Xiaoyu Wei[1,2], Xuhua Jian[3], Jiajun Xie[4], Rui Chen[2], Xiaodan Li[2], Zhicheng Du[5], Xiaomei Zhong[2], Jinglei Li[2], Xiaobing Zhou[2], Guanmin Ren[2], Yingjie Mei[6], Hui Liu[1,2]

[1]School of Medicine, South China University of Technology, Guangzhou, China; [2]Department of Radiology, Guangdong Provincial People's Hospital, Guangdong Academy of Medical Sciences, Guangzhou, China; [3]Department of Cardiac Surgery, Guangdong Cardiovascular Institute, Guangdong Provincial People's Hospital, Guangdong Academy of Medical Sciences, Guangzhou, China; [4]Department of Radiology, Guangzhou First People's Hospital, School of Medicine, South China University of Technology, Guangzhou, China; [5]Department of Medical Statistics, School of Public Health, Sun Yat-sen University, Guangzhou, China; [6]Philips Healthcare, Guangzhou, China

Contributions: (I) Conception and design: H Liu, X Wei; (II) Administrative support: H Liu, X Jian; (III) Provision of study materials or patients: X Jian, J Xie, H Liu; (IV) Collection and assembly of data: X Li, X Zhong, J Li, X Zhou, G Ren; (V) Data analysis and interpretation: R Chen, Z Du, X Wei; (VI) Manuscript writing: All authors; (VII) Final approval of manuscript: All authors.

Correspondence to: Hui Liu, MD. Professor of Radiology, 106 Zhong Shan Er Lu, Guangzhou 510080, China. Email: liuhuijiujiu@gmail.com.

Background: Left ventricular (LV) extracellular remodeling is a critical process in aortic stenosis (AS), which is related to functional abnormalities. Data regarding the use of combined T1 mapping and feature tracking (FT) to assess LV extracellular remodeling in severe AS are scarce. This study aimed to investigate the ability of T1-derived and FT-derived parameters to identify and assess the changes in process of LV extracellular remodeling in patients with severe AS.

Methods: A total of 49 patients with severe AS and 20 healthy volunteers were prospectively recruited. Modified look-locker inversion-recovery T1 mapping and FT imaging were performed in all participants using 3.0-T cardiac magnetic resonance imaging. The degree of myocardial fibrosis was quantified using Masson trichrome stain in biopsy specimens obtained intraoperatively from 13 patients and expressed as collagen volume fraction (CVF). Patients were divided into subgroups according to preserved LV ejection fraction (LVEF) (LVEF ≥50%) or reduced LVEF (LVEF <50%).

Results: Regarding the diffuse fibrosis burden, extracellular volume (ECV) was statistically insignificant between patients with preserved LVEF) and controls (28.0%±3.3% *vs.* 26.5%±2.3%, P>0.05). ECV in the reduced LVEF group (n=20) was significantly higher than that in the preserved LVEF group (n=29) (30.4%±3.9% *vs.* 28.0%±3.3%, P<0.05). Regarding the myocardial strain, global longitudinal strain (GLS) showed increasing impairment from the control group to the preserved LVEF AS group to the reduced LVEF AS group (−23.4%±3.3% *vs.* −18.6%±3.8% *vs.* −11.2%±4.8%, P<0.05). A significant correlation was found between ECV and CVF (r=0.64, P=0.020), whereas the correlation between GLS and CVF was insignificant. Significant correlations were observed between GLS and LV mass index (r=0.72, P=0.006) and LVEF (r=0.82, P<0.001). However, no correlations were found between ECV and LV mass index (P=0.172) and between ECV and LVEF (P=0.339). Discrimination of patients with preserved LVEF from controls, GLS yielded the best diagnostic performance as defined by the area of under the curve (−0.83), and GLS, ECV, and post-T1 were significant discriminators after regression analysis.

Conclusions: In the process of LV extracellular remodeling in severe AS, ECV is the structural marker of extracellular fibrosis burden, and GLS is the functional marker before the fibrosis burden intensifies.

Keywords: T1 mapping; feature tracking (FT); aortic stenosis (AS); extracellular remodeling; cardiac magnetic resonance (CMR)

Introduction

Aortic stenosis (AS) is the most common valvular disease, with a growing prevalence in the aging population (1). In response to the narrowed valve, left ventricular (LV) hypertrophy is initially adaptive to restore wall stress and cardiac function. Ultimately, LV decompensation occurs as symptoms, followed by heart failure and death (2). The transition from adaptation to decompensation is mainly driven by LV remodeling (3,4). The extracellular matrix remodeling, mostly caused by diffuse interstitial fibrosis and/or focal replacement fibrosis, is the critical process of LV remodeling (5). Consequently, researchers are extensively interested in identifying and developing objective markers to detect structural and functional changes in the process of LV extracellular remodeling.

Cardiac magnetic resonance (CMR) imaging allows the comprehensive assessment of LV remodeling with its unlimited windows and excellent myocardial tissue characterization (6). CMR imaging can detect replacement myocardial fibrosis (MF) with late gadolinium enhancement (LGE) and detect diffuse interstitial fibrosis with the T1 mapping technique. T1 mapping-derived extracellular volume (ECV) has been reported as a promising marker for assessing diffuse MF in patients with AS (5,7). Both cellular hypertrophy and extracellular fibrosis can contribute to abnormal myocardial mechanics. Recently, myocardial deformation imaging assessed by echocardiography and/or CMR imaging has gradually become a valuable and noninvasive tool to reflect intrinsic myocardial contractility and functional consequences of related cardiac diseases (8). Although deformation imaging has been used to analyze MF and myocardial remodeling in various cardiac conditions (9-12), it was seldom reported in AS by the CMR-feature tracking (FT) technique. Furthermore, data regarding the utility of combined CMR T1 mapping and FT imaging for assessing the process of LV extracellular remodeling in AS are scarce.

The purpose of this study was to investigate the ability of CMR imaging parameters to identify and assess the changes in the process of LV extracellular remodeling in patients with severe AS using the T1 mapping and FT techniques. We present the following article in accordance with the STROBE (Strengthening the Reporting of Observational Studies in Epidemiology) reporting checklist, and MDAR reporting checklist (available at http://dx.doi.org/10.21037/cdt-20-803).

Methods

Study population

Patients with severe AS were prospectively and consecutively recruited from January 2018 to June 2019 in a single tertiary center. The inclusion criteria for the patient group were as follows (should meet two or more criteria): mean transvalvular pressure gradient (MPG) ≥50 mmHg, peak pressure difference gradient (PPG) ≥70 mmHg, and/or aortic valvular area (AVA) ≤1.0 cm^2 as detected using echocardiography following guidelines (13). The exclusion criteria were as follows: moderate or severe concomitant valvular disease, history of myocardial infarction or acute coronary syndrome, contraindications to CMR imaging, and estimated glomerular filtration rate <30 mL/min/1.73 m^2. Twenty healthy volunteers who were recruited from the community without cardiovascular disease were selected as controls. This study conformed to the ethical guidelines of the Declaration of Helsinki (as revised in 2013) and was approved by the Guangdong Provincial People's Hospital, Guangdong Academy of Medical Sciences ethics committee (No. 20170216). Written informed consent was obtained from all participants.

Echocardiography

Transthoracic echocardiography was performed using a GE Vivid 9 (GE Vingmed Ultrasound, Horten, Norway) with an M5S probe (2–4 MHz) following the guidelines of the European Society of Echocardiography (14). Flow velocity across the aortic valve was measured at multiple transducer positions using continuous-wave Doppler. MPG and PPG were calculated with a simplified Bernoulli equation. AVA and AVA index was calculated using the continuity equation.

CMR imaging acquisition

All studies were performed on a 3.0-T magnetic resonance imaging scanner (Ingenia, Philips Medical Systems, Best, the Netherlands) using a standard clinical scan protocol. For cine imaging, a stack of short-axis single-shot balanced standard steady-state free-precession sequence images from the apex to the base were collected along with long-axis planes (two-, three-, and four-chamber views). The cine imaging parameters were as follows: field of view, 230×230 mm^2; voxels, 2×2×8 mm^3; TR, shortest; TE, shortest; sense factor, 2; minimum inversion time, 105 ms;

and flip angle, 45°.

T1 mapping was performed with a modified look-locked inversion-recovery sequence in three short-axis slices, including basal, mid-, and apical ventricular planes. For pre-contrast, a 5s(3s)3s scheme was used. A total dose of 0.2 mmol/kg gadopentetate dimeglumine injection (Consun Pharmaceutical Co., Ltd.) was administered. For post-contrast, a 4s(1s)3s(1s)2s scheme was used approximately 15–17 min after the contrast ejection. The T1 mapping imaging parameters were as follows: field of view, 230×230 mm^2; voxels, 2×2×8 mm^3; TR, shortest; TE, shortest; sense factor, 2; minimum inversion time, 105 ms; and flip angle, 20°.

LGE imaging was performed using a phase-sensitive inversion-recovery (PSIR) sequence approximately 10–11 min after contrast ejection, covering a stack of short-axis images from the apex to the base along with long-axis planes (two-, three-, and four-chamber views). The PSIR imaging parameters were as follows: field of view, 230×230 mm^2; voxels, 2×2×8 mm^3; TR, shortest; TE, shortest; and TI, measured at that time.

CMR imaging analysis

LV volume, function, and LGE were analyzed offline using the QMASS software (Version 2.0, Medis, Leiden, the Netherlands). LGE extent was quantified using a signal intensity threshold level of five standard deviations (SDs), and expressed in grams and derived as a percentage of LV. For T1 mapping, myocardial T1 times were measured carefully in a global region of interest (ROI) at the whole mid-ventricular wall by sketching the endocardial and epicardial borders. Meanwhile, an ROI was drawn in the LV cavity to measure the blood pool T1 time (Figure S1). Areas with LGE were not excluded from T1 analysis. T1 mapping was calculated using the MapMarker software (Version 2.0, Medis, Leiden, the Netherlands). The λ and ECV were calculated as follows:

$$\lambda = [\frac{1}{myo\ post\ T1} - \frac{1}{myo\ native\ T1}] / [\frac{1}{blood\ post\ T1} - \frac{1}{blood\ native\ T1}] \quad [1]$$

$$ECV = (1 - hematocrit) * [\frac{1}{myo\ post\ T1} - \frac{1}{myo\ native\ T1}] / [\frac{1}{blood\ post\ T1} - \frac{1}{blood\ native\ T1}] \quad [2]$$

LV myocardial strain and strain rate analysis were evaluated by loading cine SSFP images the into the tissue tracking module (QStrain 2.0, Medis, Leiden, the Netherlands) using two-dimensional (2D) FT technique. The LV's endocardial and epicardial borders were manually sketched in the end-diastolic and end-systolic phases, respectively (Figure S2). Trabeculations were all excluded from the endocardial borders. Global longitudinal strain (GLS) and strain rate were obtained from two-, three-, and four-chamber views for LV. Global circumferential strain (GCS), global radial strain (GRS), and strain rate were obtained from the LV's basal, middle, and apical levels in the short-axis view.

Patients were divided into subgroups according to preserved LVEF (LVEF ≥50%) or reduced LVEF (LVEF% <50%). The intraobserver and interobserver reproducibility were tested in randomly selected 21 patients and 9 controls for measuring T1-derived and FT-derived parameters by 2 blinded investigators (with 5 and 12 years of CMR imaging experience).

LV myocardial biopsy

Thirteen patients with severe AS underwent myocardial biopsy at aortic valve replacement (AVR) surgery. Two to four biopsy samples from the septum were gathered, stained with hematoxylin-eosin and Masson trichome strain, and used for histopathological examination under a high-power microscope (Microscope BX-51-32F01, Olympus, ×200). The quantification of histologic fibrosis was performed using ImageJ software (http://rsb.info.nih.gov/ij) and expressed as collagen volume fraction (CVF). Five different histological slices were analyzed and averaged to quantify extracellular fibrosis burden.

Statistical analysis

Statistical analyses were conducted using SPSS version 17.0 software (IBM Inc., IL, USA) and MedCalc Statistical Software version 19.0.7 (MedCalc Software bvba, Ostend, Belgium). Normality was checked using the Shapiro-Wilk test. Continuous variables were expressed as mean ± standard deviation. Categorical variables were expressed as numbers and percentages. Groups were compared using the unpaired-sample *t*-test and chi-square test, as appropriate. The relationship between two continuous variables was assessed using simple linear regression. The strength of correlation was presented as a Pearson

Table 1 Baseline characteristics of patients with severe AS

Characteristic	Severe AS (n=49)
Age, year	58.3±11
Male, %	20 [41]
Body surface area, m^2	1.7±0.12
Heart rate, bpm	80±12
Cause of AS (% of bicuspid)	29 [59]
Comorbidities	
Hypertension	9 [18.4]
Systolic BP, mmHg	122±25
Diastolic BP, mmHg	72±13
Diabetes mellitus	1 [2]
Hyperlipidemia	7 [14]
Symptoms	
Angina	29 [59]
Syncope	0 [0]
Dyspnea	15 [31]
Blood	
Creatinine, mg/mL	83.2±20.5
NT-proBNP, pg/mL	2168.8±2788.8
Hematocrit, %	38±5.4
Echocardiography	
Mean pressure gradient of AV, mmHg	65.5±19.3
Peak pressure gradient of AV, mmHg	106.5±29.1
AVA, cm^2	0.9±0.2
AVA index, cm^2/m^2	0.5±0.1
AVR	43 [88]

Values are mean ± SD or n [%]. AS, aortic stenosis; BP, blood pressure; NT-proBNP, N-terminal pro-B-type natriuretic peptide; AV, aortic valve; AVA, aortic valve area; AVR, aortic valve replacement.

correlation coefficient. Univariate and multivariate binary logistic regression by the stepwise backward method was used to test the ability of CMR imaging measures to discriminate patients with preserved LV ejection fraction (LVEF) from healthy controls. The sensitivity, specificity, discrimination threshold, and area under the curve (AUC) were calculated using receiver operating characteristics curve (ROC) analysis. The intraclass correlation coefficient

(ICC) and Bland-Altman plots were used to assess inter- and intraobserver reproducibility. A two-sided P value <0.05 was considered significant.

Results

Baseline characteristics

The demographic data of patients with severe AS are shown in *Table 1*. A total of 49 patients with severe AS (58.3±11 years; 20 male) were included; of these, 43 patients (43/49, 88%) had AVR. The bicuspid was the most common cause of AS (29/49, 59%). Regarding the echocardiographic indices of stenosis of the aortic valve, the MPG, PPG, AVA, and AVA index were 65.5±19.3 mmHg, 106.5±29.1 mmHg, 0.9±0.2 cm^2, and 0.5±0.1 cm^2/m^2, respectively.

CMR imaging findings

The CMR imaging findings are summarized in *Table 2*. An increasing gradient of LV volume (LV end-diastolic index: 82.6±9.1 *vs.* 100.8±24.1 *vs.* 146.1±48.6 mL/m^2, P<0.05; LV end-systolic index: 30.2±6.7 *vs.* 39.7±12.2 *vs.* 98.0±46.2 mL/m^2, P<0.05) and hypertrophy (LV mass index: 37.4±7.2 *vs.* 85.7±24.1 *vs.* 125.1±38.4 g/m^2, P<0.05) indices was observed from the control group (n=20) to the preserved LVEF AS group (n=29) to the reduced LVEF AS group (n=20). However, the LVEF (35.1%±11.1% *vs.* 61.1%±4.9%, P<0.001) and stroke volume (SV) index (48.2±15.0 *vs.* 61.2±13.6 mL/m^2, P<0.01) of LV systolic function both decreased in patients with reduced LVEF group compared with the preserved LVEF group.

Regarding the parameters of fibrosis imaging, focal displacement fibrosis measured by LGE was detected in 28 patients (28/49, 57%) with infarct-like and/or non-infarct two patterns. There was no statistically significant difference in focal displacement fibrosis burden between patients with preserved LVEF and reduced LVEF groups (LGE%: 6.4%±3.7% *vs.* 6.6%±2.5%, P>0.05). For the diffuse fibrosis burden, the native T1 and ECV values estimated by T1 mapping was significantly higher in the reduced LVEF group than in the preserved LVEF group (1,357.8±46.5 *vs.* 1,299.6±41.0 ms, P<0.001; 30.4%±3.9% *vs.* 28.0%±3.3%, P<0.05), and higher than that in the healthy controls (1,357.8±46.5 *vs.* 1,281.6±29.5 ms, P<0.001; 30.4%±3.9% *vs.* 26.5%±2.3%, P<0.01). However, the native T1 and ECV values were statistically insignificant between patients with preserved LVEF and healthy controls (1,299.6±41.0 *vs.*

Table 2 CMR parameters in patients with severe AS and controls

Characteristic	Control subjects (n=20)	Patients with preserved LVEF (n=29)	Patients with reduced LVEF (n=20)
LVEDV index, mL/m^2	82.6±9.1	100.8±24.1**	146.1±48.6$^{\#\#***}$
LVESV index, mL/m^2	30.2±6.7	39.7±12.2**	98.0±46.2$^{\#\#\#***}$
LVEF, %	62.8±6.4	61.1±4.9	35.1±11.1$^{\#\#\#***}$
SV index, mL/m^2	52.3±7.3	61.2±13.6**	48.2±15.0$^{\#\#}$
CI, L/min per m^2	3.7±0.7	4.5±0.9**	4.0±1.2
LVM index, g/m^2	37.4±7.2	85.7±24.1***	125.1±38.4$^{\#\#\#***}$
Mass/volume ratio, g/mL	0.5±0.1	0.9±0.2***	0.9±0.3***
LV MWT, mm	9.7±1.4	17.7±3.6***	18.4±5.4***
LGE (n, %)	–	14 [48]	14 [70]
LGE mass, g	–	8.6±5.9	13.1±5.7
LGE %	–	6.4±3.7	6.6±2.5
T1 mapping parameters			
Native T1 value, ms	1,281.6±29.5	1,299.6±41.0	1,357.8±46.5$^{\#\#\#***}$
Post T1 value, ms	565.3±59.9	527.8±71.7	576.5±53.9$^{\#}$
λ	0.45±0.0	0.46±0.0	0.5±0.1$^{\#\#***}$
ECV value, %	26.5±2.3	28.0±3.3	30.4±3.9$^{\#***}$
Stain parameters			
GLS, %	−23.4±3.3	−18.6±3.8***	−11.2±4.8$^{\#\#\#***}$
GCS, %	−24.6±3.5	−19.8±3.7***	−12.6±5.0$^{\#\#\#***}$
GRS, %	101.7±30.2	78.3±26.3**	40.5±27.3$^{\#\#\#***}$
GLS rate	−1.00±0.2	−0.8±0.2**	−0.5±0.2$^{\#\#\#***}$
GCS rate	−1.0±0.2	−0.9±0.2	−0.6±0.5$^{\#***}$
GRS rate	2.0±0.5	3.2±6.3	1.4±1.2

Values are mean ± SD or n [%]. Statistical significance was defined as P<0.05. **, P<0.001; ***, P<0.001 versus controls. $^{\#}$, P<0.05; $^{\#\#}$, P<0.01; $^{\#\#\#}$, P<0.001 versus patients with preserved LVEF%. CMR, cardiac magnetic resonance; AS, aortic stenosis; LVEDV, left ventricular end diastolic volume; LVESV, left ventricular end systolic volume; LVEF, left ventricular ejection fraction; SV, stroke volume; CI, cardiac index; LVM, left ventricular mass; MWT, maximum wall thickness; LGE, late gadolinium enhancement; ECV, extracellular volume; GLS, global longitudinal strain; GCS, global circumferential strain; GRS, global radial strain.

1,281.6±29.5 ms, P>0.05; 28.0%±3.3% *vs.* 26.5%±2.3%, P>0.05).

Regarding the strain parameters of FT, the values of global longitudinal strain (GLS) (−23.4%±3.3% *vs.* −18.6%±3.8% *vs.* −11.2%±4.8%, P<0.05), circumferential strain (GCS) (−24.6%±3.5% *vs.* −19.8%±3.7% *vs.* −12.6%±5.0%, P<0.05), and radial strain (GRS) (101.7%±30.2% *vs.* 78.3%±26.3% *vs.* 40.5%±27.3%, P<0.05) values showed increasing impairment from the control group to the preserved LVEF AS group to the reduced LVEF AS group.

Analysis of relationships

A significant linear correlation was found between ECV and CVF (r=0.64, P=0.020). However, the correlation between GLS and CVF was insignificant (P=0.538) (*Figure 1*). Linear correlation analysis between ECV/GLS and global LV structural/functional parameters in patients with severe AS (*Figure 2*) revealed significant correlations between GLS and LVMi (r=0.072, P=0.006) and between GLS and LVEF (r=−0.83, P<0.001). However, no significant correlations were observed between ECV and LVMi (P=0.172) and
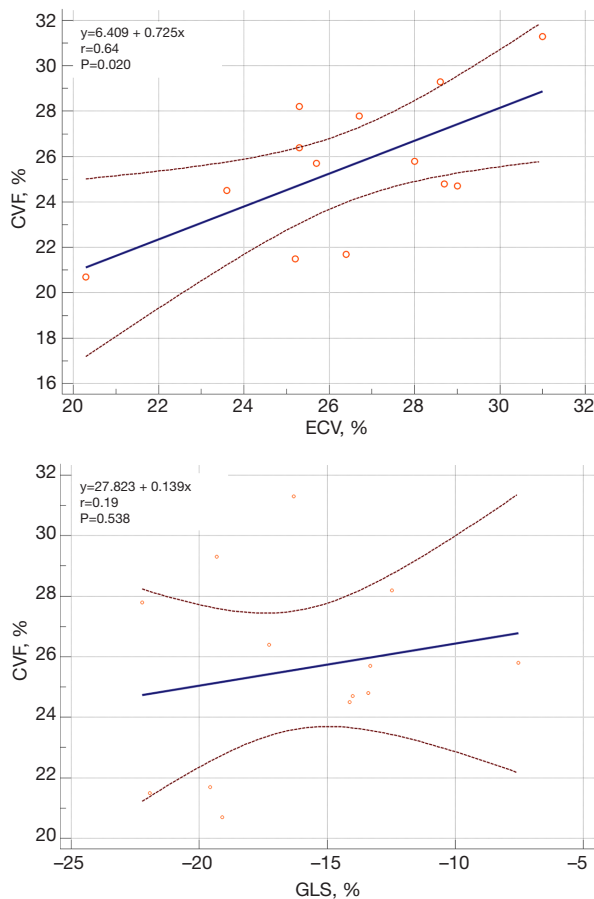
Figure 1 Correlation of CVF with ECV and GLS in patients with severe AS. The analysis showed a moderate correlation between ECV and CVF (r=0.64, P=0.020). However, no significant correlation was found between GLS and CVF (P=0.538). The dotted line represents the 95% confidence interval. CVF, collagen volume fraction; ECV, extracellular volume fraction; GLS, global longitudinal strain; AS, aortic stenosis.

between ECV and LVEF (P=0.339).

Discrimination of patients with preserved LVEF from controls

GLS yielded the best diagnostic performance as defined by AUC (0.83), followed by GCS (0.82), GLS rate (0.79), post T1 (0.71), and GRS (0.71), in discriminating patients with preserved LVEF from healthy controls. The discriminatory values of other parameters are summarized in *Table 3*. The GLS [Exp (B): 1.46, 95% confidence interval (CI): 1.16–1.85, P=0.002], ECV [Exp (B): 1.40, 95% CI: 1.02–1.90,

P=0.035], and post T1 [Exp (B): 0.98, 95% CI: 0.79–0.99, P=0.042] were the significant parameters in discriminating patients with preserved LVEF from healthy controls. Univariate and multivariate binary logistic regression results are presented in *Table 4*.

Intraobserver and interobserver reproducibility

The intraobserver and interobserver reproducibility of T1-derived and global LV strain parameters were calculated and assessed. Excellent intraobserver reproducibility was found for GLS (ICC =0.91; 95% CI: 0.83 to 0.96) and ECV (ICC =0.90; 95% CI: 0.81 to 0.95). Excellent interobserver reproducibility was found for GLS (ICC =0.91; 95% CI: 0.82 to 0.96) and slightly excellent interobserver reproducibility for ECV (ICC =0.86; 95% CI: 0.73 to 0.93). The results of ICCs are summarized in *Table 5*, and those of Bland-Altman plots are shown in *Figure 3* and Figure S3.

Discussion

The principal findings of the present study were as follows: (I) GLS was the functional marker of extracellular remodeling, which showed significant correlations between GLS and LVEF (r=−0.83, P<0.001). (II) GLS is the functional marker of myocardial mechanics related to disease state before the fibrosis burden intensifies. It showed increasing impairment from the control group to the preserved LVEF AS group to the reduced LVEF AS group (−23.4%±3.3% *vs.* −18.6%±3.8% *vs.* −11.2±4.8%, P<0.05), and showed the best diagnostic performance (AUC 0.83) as a significant discriminator between patients with preserved LVEF and controls. (III) ECV was the structural marker of extracellular diffuse fibrosis burden, which showed a significant correlation between ECV and CVF (r=0.64, P=0.020).

Myocardial deformation imaging has been reported as a sensitive modality to evaluate the functional consequences of MF (8,15). The LV function is determined by the sum of contraction and relaxation in the endo-, mid-, and epicardial layers. Therefore, the myocardial dysfunction in the involved myocardial layer can be classified into subendocardial, transmural, and subepicardial myocardial dysfunction (16). During the course of AS, the early stage of MF starts in the subendocardial layers leading to a reduction in longitudinal LV mechanics (17). However, LVEF, which is predominantly determined by mid-MF, can be normal even in the presence of extensive subendocardial
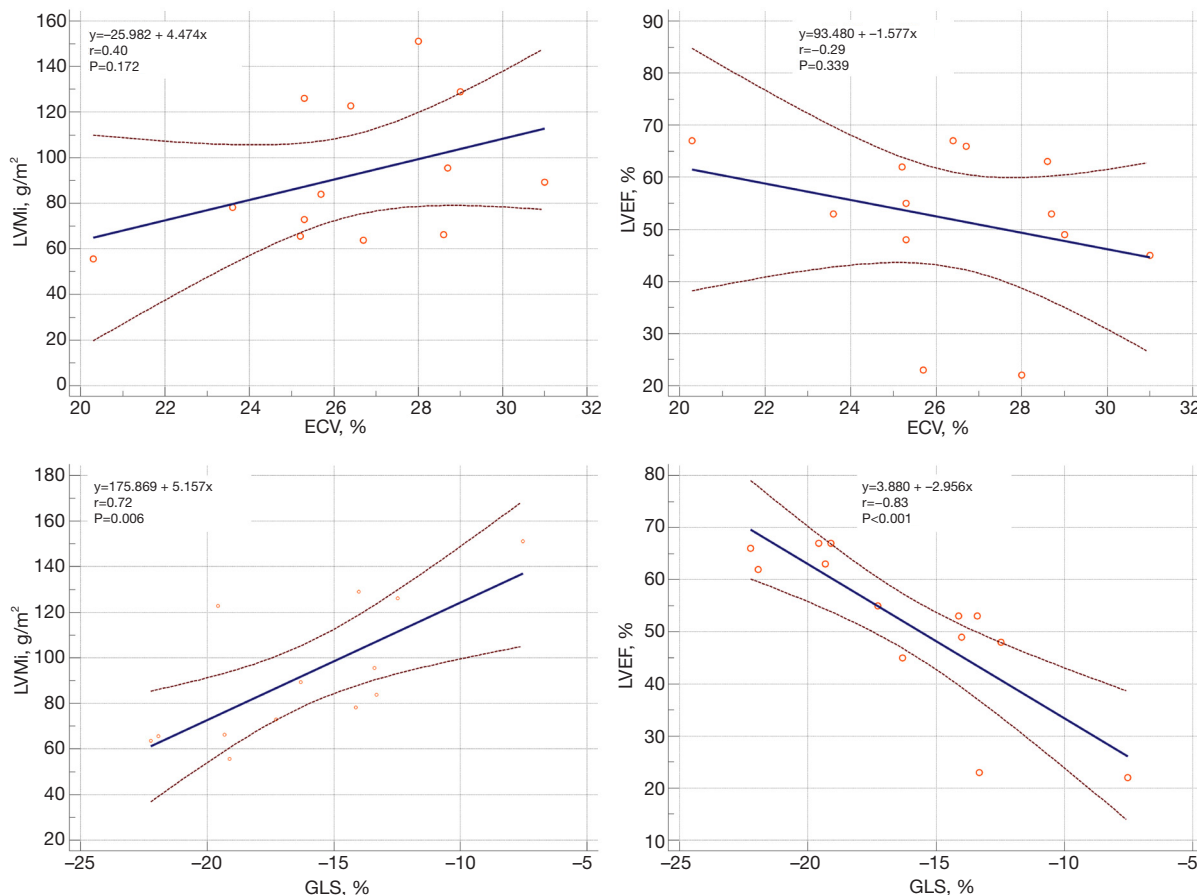
Figure 2 Correlation between ECV/GLS and global LV structural/functional parameters in patients with severe AS. The analysis showed significant correlations between GLS and LVMi (r=0.072, P=0.006) and between GLS and LVEF (r=−0.83, P<0.001). However, no significant correlations were observed between ECV and LVMi (P=0.172) and between ECV and LVEF (P=0.339). The dotted line represents the 95% confidence interval. ECV, extracellular volume fraction; GLS, global longitudinal strain; AS, aortic stenosis; LV, left ventricular; LVEF, left ventricular ejection fraction.

Table 3 ROC analysis of T1-derived and FT-derived biomarkers for discrimination between patients with severe AS with preserved LVEF and controls

Biomarkers	AUC (95% CI)	Discrimination threshold	Sensitivity (%)	Specificity (%)
Native T1, ms	0.68 (0.53–0.81)	>1,298.4	55.2	85.0
Post T1, ms	0.71 (0.57–0.83)	≤566.7	72.4	70.0
λ	0.55 (0.40–0.69)	≤0.41	24.1	95.0
ECV, %	0.64 (0.49–0.77)	>26.6	69.0	65.0
GLS, %	0.83 (0.70–0.92)	>−19.9	72.4	85.0
GCS, %	0.82 (0.69–0.92)	>−21.5	65.5	90.0
GRS, %	0.71 (0.56–0.83)	≤92.7	69.0	65.0
GLS rate	0.79 (0.65–0.90)	>−0.9	79.3	75.0
GCS rate	0.62 (0.47–0.76)	>−0.97	65.5	60.0
GRS rate	0.53 (0.39–0.68)	≤1.6	44.8	80.0

LVEF, left ventricular ejection fraction; ROC, receive operating curve; AUC area under the curve; ECV, extracellular volume; GLS, global longitudinal strain; GCS, global circumferential strain; GRS, global radial strain.

Table 4 Binary logistic regression analysis of T1-derived and FT-derived biomarkers for discrimination between patients with severe AS with preserved LVEF and controls

Variable	Univariate analysis		Multivariate analysis	
	Exp(B) (95% CI)	P value	Exp(B) (95% CI)	P value
Native T1, ms	1.01 (0.99–1.03)	0.107		
Post T1, ms	0.99 (0.98–1.00)	0.070	0.98 (0.97–0.99)	0.042
λ	0.13 (0.01–556.89)	0.756		
ECV, %	1.20 (0.97–1.48)	0.096	1.40 (1.02–1.90)	0.035
GLS, %	1.43 (1.16–1.76)	0.001	1.46 (1.16–1.85)	0.002
GCS, %	1.45 (1.16–1.81)	0.001		
GRS, %	0.97 (0.95–0.99)	0.011		
GLS rate	238.76 (6.41–8888.66)	0.003		
GCS rate	8.61 (0.54–138.70)	0.129		
GRS rate	1.16 (0.68–1.98)	0.590		

The imaging biomarker of P<0.1 in the univariate analysis entered the multivariate analysis. AS, aortic stenosis; LVEF, left ventricular ejection fraction; ECV, extracellular volume; GLS, global longitudinal strain; GCS, global circumferential strain; GRS, global radial strain.

Table 5 Intraobserver and interobserver reproducibility

Variable	Intraobserver reproducibility			Interobserver reproducibility		
	ICC	95% CI	Bias	ICC	95% CI	Bias
Native T1	0.93	0.87–0.97	−0.90±15.51	0.94	0.87–0.97	−14.64±15.90
Post T1	0.93	0.86–0.97	22.16±29.23	0.93	0.86–0.97	−4.63±27.42
ECV	0.90	0.81–0.95	1.23±1.31	0.86	0.73–0.93	−1.63±1.61
GLS	0.91	0.83–0.96	−0.43±2.01	0.91	0.82–0.96	−0.02±1.90
GCS	0.93	0.87–0.97	−0.52±1.66	0.85	0.71–0.93	−0.89±2.38
GRS	0.64	0.37–0.90	−4.89±26.63	0.44	0.10–0.69	−6.92±30.56

ICC, intraclass correlation coefficient; CI, confidence interval; ECV, extracellular volume; GLS, global longitudinal strain; GCS, global circumferential strain; GRS, global radial strain.

fibrosis (3,18). Consistent with previous studies using the echocardiographic technique (19-21), the present study demonstrated a reduction in GLS in patients with AS compared with controls despite a preserved LVEF using the CMR-FT technique. These findings suggested that GLS might better characterize subtle mechanical changes in LV during the remodeling process in patients with AS and that GLS had an earlier diagnostic power than LVEF in this clinical setting. Furthermore, the present study showed that GLS, GCS, and GRS were increasingly impaired from the control group to the preserved LVEF AS group to the reduced LVEF AS groups, which indicated

that subtle changes in longitudinal and radial deformation were gradually related to the disease state. Thus, an objective change in myocardial strain is more sensitive than observable symptoms and general functional parameters (e.g., LVEF and SV) in detecting a functional abnormality in AS.

GLS has been validated as a sensitive parameter in quantifying longitudinal LV function, which is more reproducible and less variable than other deformation indices in line with the results of reproducibility in the present study. CMR imaging strain parameters derived from FT could reflect early functional change using routine cine
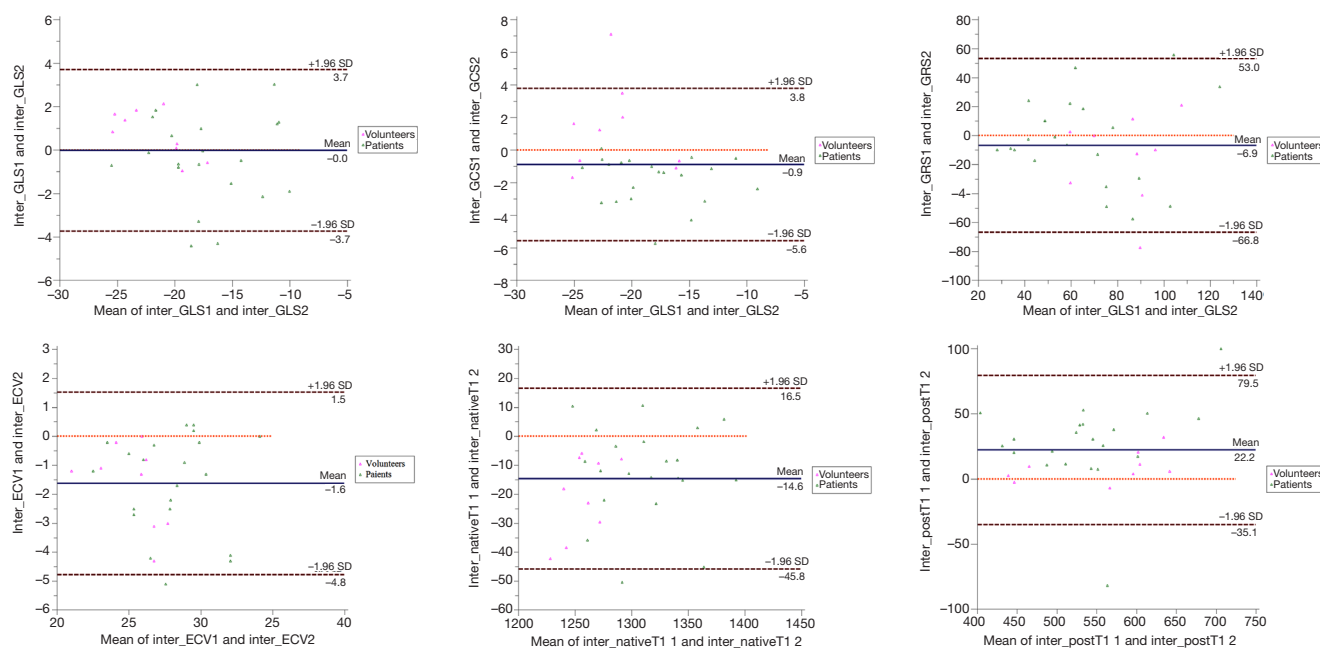
Figure 3 Reproducibility of CMR-FT and T1 mapping parameters. Bland-Altman plots showed interobserver agreement for CMR-FT-derived GLS, GCS, and GRS parameters, and for T1-derived ECV, native T1, and post T1 parameters in selected participants (n=30). CMR, cardiac magnetic resonance; ECV, extracellular volume fraction; GCS, global circumferential strain; GRS, global radial strain.

images in less than 10 min (22). As a simple and practical method, GLS acquired from FT is a promising technique in assessing functional consequences in the subclinical stage of severe AS, especially in patients with suboptimal echocardiographic image quality.

T1 mapping–derived ECV has emerged as a novel and promising marker to evaluate diffuse MF due to better histopathological correlation in the studies by Park (23) (r=0.645, P<0.001) and Chin (24) (r=0.70, P=0.016), in line with the findings of the present study (r=0.64, P=0.020). With regards to LV structure and function, no significant correlation of ECV with LVMi and LVEF was found, consistent with the study by Treibel (18), which showed that ECV correlated weakly with LVEF (r²=−0.096, P=0.001) and did not correlate with LVMi (P=0.06). However, a strong correlation of GLS with LV structure (LVMi) and function (LVEF) was found in the present study. Therefore, the ECV obtained using T1 mapping could be an ideal surrogate marker for detecting extracellular diffuse fibrosis burden but not be a sensitive marker for assessing the functional changes in LV extracellular remodeling.

A comparison of the control group with the preserved LVEF AS and reduced LVEF AS groups in the present study showed that GLS was an early marker of myocardial

mechanics related to the disease state before the fibrosis burden intensified. When no difference was observed in extracellular fibrosis burden (ECV) between patients with preserved LVEF and controls, global LV strain parameters (e.g., GLS and GCS) had been impaired. This finding suggested that functional changes might be manifested before structural changes. Further studies on myocardial biopsy specimens from more early-stage and asymptomatic patients are needed to verify the findings.

This study had several limitations. First, this was a single-center cohort study with a small sample size. Hence, further larger-scale investigations are needed. Second, although the histopathological analysis (the gold standard for assessing fibrosis) was performed in some patients, the sample size was still small. Third, the present study using combined T1 mapping and FT techniques lacked follow-up and prognostic information. Studies with long-term follow-up are required to validate and expand the findings of this study in the future.

Conclusions

In the process of LV extracellular remodeling in severe AS, ECV is the structural marker of extracellular fibrosis

1856

Wei et al. T1 mapping and FT of LV extracellular remodeling in AS

burden, and GLS is the functional marker before the fibrosis burden intensifies. Although large-scale clinical studies are needed, the results suggested that the GLS and ECV must be combined to assess the process of LV extracellular remodeling to optimize clinical strategy and improve patient prognosis.

Acknowledgments

Footnote

Reporting Checklist: The authors have completed the STROBE reporting checklist and MDAR reporting checklist. Available at http://dx.doi.org/10.21037/cdt-20-803

Data Sharing Statement: Available at http://dx.doi.org/10.21037/cdt-20-803

Peer Review File: Available at http://dx.doi.org/10.21037/cdt-20-803

Conflicts of Interest: All authors have completed the ICMJE uniform disclosure form (available at http://dx.doi.org/10.21037/cdt-20-803). The authors have no conflicts of interest to declare.

Ethical Statement: The authors are accountable for all aspects of the study in ensuring that questions related to the accuracy or integrity of any part of the study are appropriately investigated and resolved. The research was conducted in accordance with the Declaration of Helsinki (as revised in 2013), and was approved by the Guangdong Provincial People's Hospital, Guangdong Academy of Medical Sciences ethics committee (No.: 20170216). Written informed consent was obtained for all participants before CMR imaging.

Open Access Statement: This is an Open Access article distributed in accordance with the Creative Commons Attribution-NonCommercial-NoDerivs 4.0 International License (CC BY-NC-ND 4.0), which permits the non-commercial replication and distribution of the article with the strict proviso that no changes or edits are made and the original work is properly cited (including links to both the formal publication through the relevant DOI and the license). See: https://creativecommons.org/licenses/by-nc-nd/4.0/.

References

1. Baumgartner H, Falk V, Bax JJ, et al. 2017 ESC/EACTS Guidelines for the management of valvular heart disease. Eur Heart J 2017;38:2739-91.
2. Chin CW, Vassiliou V, Jenkins WS, et al. Markers of left ventricular decompensation in aortic stenosis. Expert Rev Cardiovasc Ther 2014;12:901-12.
3. Hein S, Arnon E, Kostin S, et al. Progression from compensated hypertrophy to failure in the pressure-overloaded human heart: structural deterioration and compensatory mechanisms. Circulation 2003;107:984-91.
4. Dweck MR, Boon NA, Newby DE. Calcific aortic stenosis: a disease of the valve and the myocardium. J Am Coll Cardiol 2012;60:1854-63.
5. Bing R, Cavalcante JL, Everett RJ, et al. Imaging and Impact of Myocardial Fibrosis in Aortic Stenosis. JACC Cardiovasc Imaging 2019;12:283-96.
6. Singh A, McCann GP. Cardiac magnetic resonance imaging for the assessment of aortic stenosis. Heart (British Cardiac Society) 2019;105:489-97.
7. Kockova R, Kacer P, Pirk J, et al. Native T1 Relaxation Time and Extracellular Volume Fraction as Accurate Markers of Diffuse Myocardial Fibrosis in Heart Valve Disease- Comparison With Targeted Left Ventricular Myocardial Biopsy. Circ J 2016;80:1202-9.
8. Claus P, Omar AMS, Pedrizzetti G, et al. Tissue Tracking Technology for Assessing Cardiac Mechanics: Principles, Normal Values, and Clinical Applications. JACC Cardiovasc Imaging 2015;8:1444-60.
9. Hwang JW, Kim SM, Park SJ, et al. Assessment of reverse remodeling predicted by myocardial deformation on tissue tracking in patients with severe aortic stenosis: a cardiovascular magnetic resonance imaging study. J Cardiovasc Magn Reson 2017;19:80.
10. Almaas VM, Haugaa KH, Strom EH, et al. Noninvasive assessment of myocardial fibrosis in patients with obstructive hypertrophic cardiomyopathy. Heart 2014;100:631-8.
11. Cameli M, Mondillo S, Righini FM, et al. Left Ventricular

Deformation and Myocardial Fibrosis in Patients With Advanced Heart Failure Requiring Transplantation. J Card Fail 2016;22:901-7.

12. Hoffmann R, Altiok E, Friedman Z, et al. Myocardial deformation imaging by two-dimensional speckle-tracking echocardiography in comparison to late gadolinium enhancement cardiac magnetic resonance for analysis of myocardial fibrosis in severe aortic stenosis. Am J Cardiol 2014;114:1083-8.

13. Nishimura RA, Otto CM, Bonow RO, et al. 2017 AHA/ACC Focused Update of the 2014 AHA/ACC Guideline for the Management of Patients With Valvular Heart Disease: A Report of the American College of Cardiology/American Heart Association Task Force on Clinical Practice Guidelines. J Am Coll Cardiol 2017;70:252-89.

14. Nishimura RA, Otto CM, Bonow RO, et al. 2017 AHA/ACC Focused Update of the 2014 AHA/ACC Guideline for the Management of Patients With Valvular Heart Disease: A Report of the American College of Cardiology/American Heart Association Task Force on Clinical Practice Guidelines. Circulation 2017;135:e1159-95.

15. Reisner SA, Lysyansky P, Agmon Y, et al. Global longitudinal strain: a novel index of left ventricular systolic function. J Am Soc Echocardiogr 2004;17:630-3.

16. Sengupta PP, Narula J. Reclassifying heart failure: predominantly subendocardial, subepicardial, and transmural. Heart Fail Clin 2008;4:379-82.

17. Heymans S, Schroen B, Vermeersch P, et al. Increased cardiac expression of tissue inhibitor of metalloproteinase-1 and tissue inhibitor of metalloproteinase-2 is related to cardiac fibrosis and dysfunction in the chronic pressure-overloaded human heart. Circulation 2005;112:1136-44.

18. Treibel TA, Lopez B, Gonzalez A, et al. Reappraising myocardial fibrosis in severe aortic stenosis: an invasive and non-invasive study in 133 patients. Eur Heart J 2018;39:699-709.

19. Kusunose K, Goodman A, Parikh R, et al. Incremental prognostic value of left ventricular global longitudinal strain in patients with aortic stenosis and preserved ejection fraction. Circ Cardiovasc Imaging 2014;7:938-45.

20. Delgado V, Tops LF, van Bommel RJ, et al. Strain analysis in patients with severe aortic stenosis and preserved left ventricular ejection fraction undergoing surgical valve replacement. Eur Heart J 2009;30:3037-47.

21. Nagata Y, Takeuchi M, Wu VC, et al. Prognostic value of LV deformation parameters using 2D and 3D speckle-tracking echocardiography in asymptomatic patients with severe aortic stenosis and preserved LV ejection fraction. JACC Cardiovasc Imaging 2015;8:235-45.

22. Pedrizzetti G, Claus P, Kilner PJ, et al. Principles of cardiovascular magnetic resonance feature tracking and echocardiographic speckle tracking for informed clinical use. J Cardiovasc Magn Reson 2016;18:51.

23. Park SJ, Cho SW, Kim SM, et al. Assessment of Myocardial Fibrosis Using Multimodality Imaging in Severe Aortic Stenosis: Comparison With Histologic Fibrosis. JACC Cardiovasc Imaging 2019;12:109-19.

24. Chin CWL, Everett RJ, Kwiecinski J, et al. Myocardial Fibrosis and Cardiac Decompensation in Aortic Stenosis. JACC Cardiovasc Imaging 2017;10:1320-33.
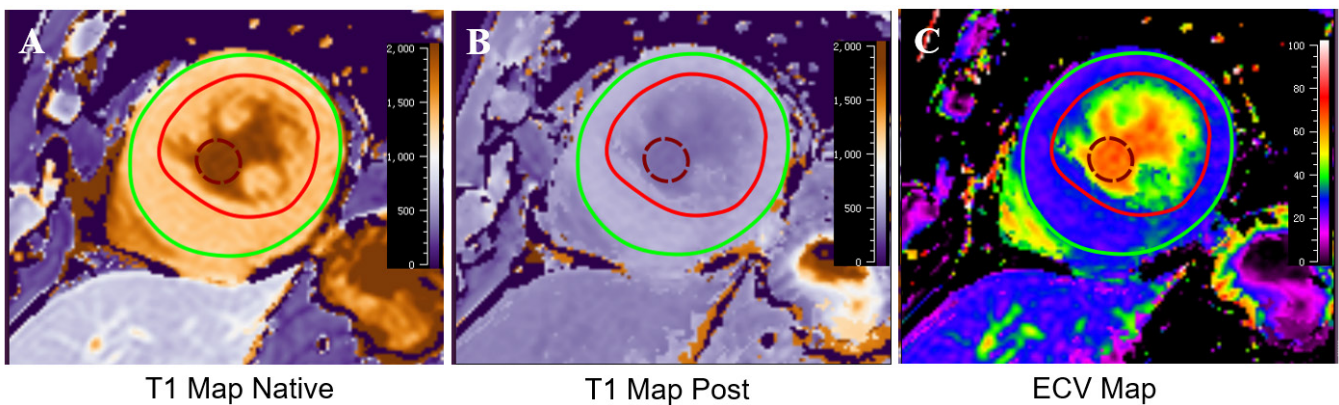
Figure S1 Measurements of native T1, post T1 and ECV mapping images in a patient with severe AS. The region of interest was drawn manually at the endo- and epi-cardial border of the mid-ventricular myocardium (red and green circles), and n at the LV cavity (red dotted circle). (A) Native T1 map with a color scale ranging from 0 (lavender) to 2000ms (brown). (B) Post contrast T1 map with color scale ranging from 0 (lavender) to 2000ms (brown). (C) ECV map ranging from 0 (purple) to 100% (red). ECV, extracellular volume.
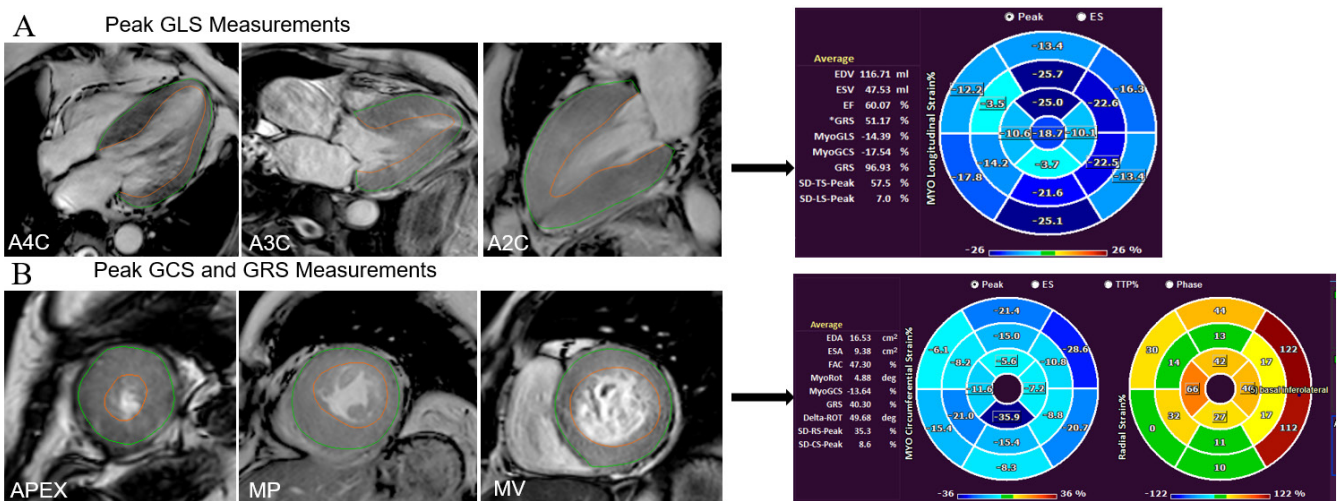

Figure S2 Measurements of feature tracking by CMR in a patient with severe AS. (A) Peak GLS was acquired by delineating endocardial and epicardial contour of A4C, A3C, and A2C in systolic and diastolic phases. (B) Peak GCS and GRS were acquired by delineating endocardial and epicardial contour of Apex, MP and MV slices in systolic and diastolic phase. A4C, apical 4 chamber; A3C, apical 3 chamber; A2C, apical 2 chamber; MP, mid plane; MV, mitral valve; GLS, global longitudinal strain; GCS, global circumferential strain; GRS, global radial strain.
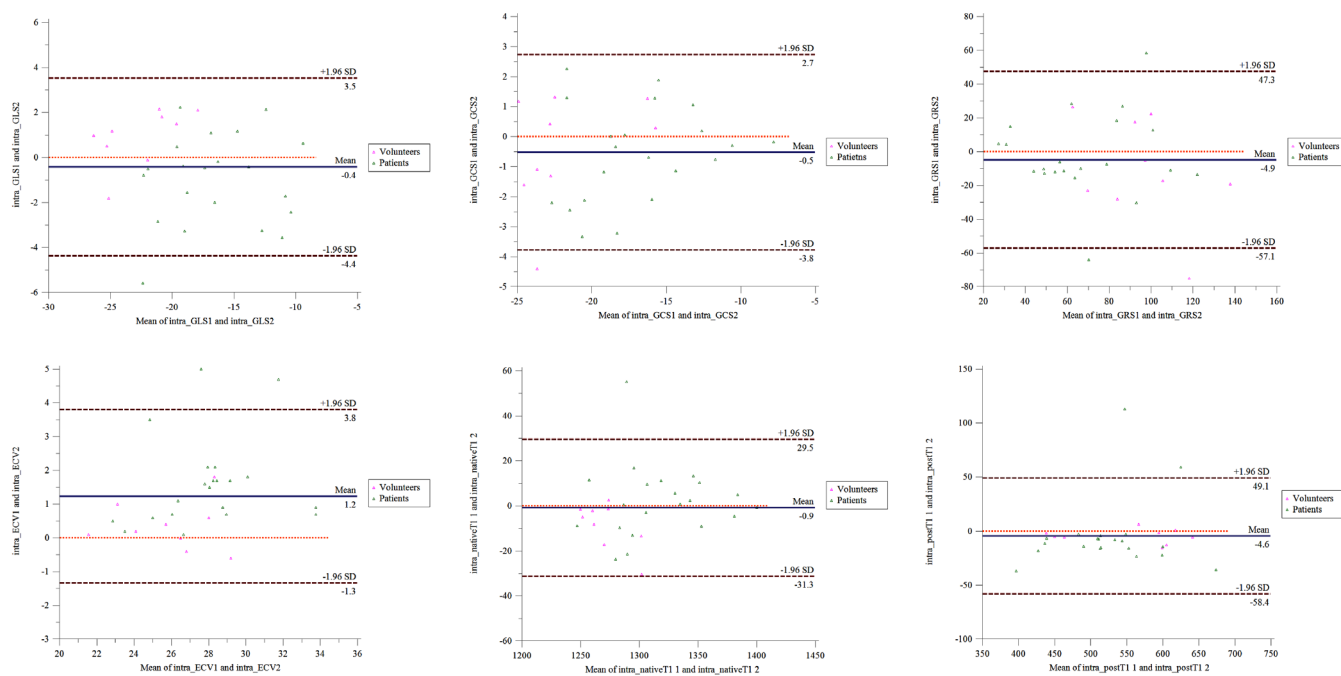
Figure S3 Reproducibility of CMR-FT and T1 mapping parameters. Bland-Altman plots showed intra-observer agreement for CMR-FT derived GLS, GCS, and GRS parameters, and for T1-derived ECV, native T1, and post T1 parameters in selected participants (n= 30). Abbreviations are shown in Supplemental Figures 1 and 2.